



AMEGHINIANA

A GONDWANAN PALEONTOLOGICAL JOURNAL



This file is an uncorrected accepted manuscript (i.e., postprint). Please be aware that during the production process this version will definitively change. This postprint will be removed once the paper is officially published.

All legal disclaimers that apply to the journal pertain.

Submitted: September 8th, 2020 – **Accepted:** November 11th, 2020 – **Posted online:** November 18th, 2020

To link and cite this article:

doi: 10.5710/AMGH.11.11.2020.3395

PLEASE SCROLL DOWN FOR ARTICLE

1 **PLANT TAPHONOMY AND PALEOENVIRONMENT OF THE BAHÍA**
2 **LAURA COMPLEX, MIDDLE-LATE JURASSIC, AT THE LAGUNA FLECHA**
3 **NEGRA LOCALITY (SANTA CRUZ PROVINCE, ARGENTINA)**

4 TAFONOMÍA DE PLANTAS Y PALEOAMBIENTE DEL COMPLEJO BAHÍA
5 LAURA, JURÁSICO MEDIO-SUPERIOR, EN LA LOCALIDAD LAGUNA
6 FLECHA NEGRA (PROVINCIA DE SANTA CRUZ, ARGENTINA)

7

8 ANA JULIA SAGASTI^{1,2}, DIEGO M. GUIDO^{2,3}, JUAN L. GARCÍA MASSINI^{3,4};
9 AND KATHLEEN A. CAMPBELL⁵

10 ¹Becaria Posdoctoral Consejo Nacional de Investigaciones Científicas y Técnicas
11 (CONICET). anajusagasti@gmail.com anajusagasti@fcnym.unlp.edu.ar

12 ²Instituto de Recursos Minerales (INREMI-UNLP), 64 nro 3, B1904AMC, La Plata,
13 Buenos Aires, Argentina.

14 ³Consejo Nacional de Investigaciones Científicas y Técnicas (CONICET), Godoy
15 Cruz 2290, CABA, Argentina.

16 ⁴Centro Regional de Investigaciones Científicas y Transferencia Tecnológica de La
17 Rioja (CRILAR-CONICET), Provincia de La Rioja, UNLaR, SEGEMAR, UNCa,
18 CONICET, Entre Ríos y Mendoza s/n, 5301, Anillaco, La Rioja, Argentina.

19 ⁵School of Environment, The University of Auckland, Private Bag 92019, Auckland
20 1142, New Zealand.

21

22 36 pages (text + references), 4 illustrations, 2 Tables

23

24 Running Header: SAGASTI *ET AL.*: PALEOENVIRONMENTAL

25 RECONSTRUCTION AT LAGUNA FLECHA NEGRA

26 Short description: Taphonomic studies allow reconstructing the depositional history and
27 plant fossilization pathways in a hot-spring (sinter) system in the Deseado Massif.

28

29 Corresponding author: Ana Julia Sagasti anajusagasti@gmail.com

30 anajusagasti@fcnym.unlp.edu.ar

31 **Abstract.** Taphonomic studies were carried out at Laguna Flecha Negra locality (Bahía
32 Laura Complex, Middle-Late Jurassic), Santa Cruz Province, Argentina. Sedimentary
33 facies and preservational styles were defined to recognize plant taphofacies in the
34 studied sequence. Eleven taphofacies were identified and plant sources within a
35 volcanic and geothermal system are proposed. Plant remains are of autochthonous to
36 para-autochthonous origin and best preservation was found in distal facies of siliceous
37 hot spring (sinter) systems. Lateral and vertical taphonomic differences were found in
38 the studied sequence. These are due to changes in the sedimentary input and distance to
39 the geothermal fluids. Results enable the reconstruction of the depositional history of
40 this region of the Deseado Massif geological Province. We infer formation of a hot-
41 spring (sinter) system that was subsequently destroyed by a phreatic eruption process at
42 the margin of an andesitic effusive dome in partially reworked fall pyroclastic subfacies.
43 After the destruction of the geothermal system, a fluvial and lacustrine epiclastic
44 subfacies developed preserving a plant community typical of the Middle-Late Jurassic
45 of Gondwana. Later, volcanic activity produced pyroclastic subfacies, with thick ash-
46 fall and flow deposits from different sources and separated by a time gap that promoted
47 fossilization of an *in situ* forest. Taphonomic studies of these plant communities
48 allowed reconstruction of a chain of geological events and how these processes have
49 influenced the preservation of a Jurassic flora from Patagonia, thus contributing to an
50 understanding of the paleoecology of the Deseado Massif geological province.

51 **Keywords.** Paleobotany. Taphonomy. Geothermal wetlands. Volcaniclastic deposits.
52 Paleoenvironmental reconstruction. Deseado Massif.

53 **Resumen.** TAFONOMÍA DE PLANTAS Y PALEOAMBIENTE DEL COMPLEJO
54 BAHÍA LAURA, JURÁSICO MEDIO-SUPERIOR, EN LA LOCALIDAD LAGUNA
55 FLECHA NEGRA (PROVINCIA DE SANTA CRUZ, ARGENTINA). Se realizó el

56 estudio tafonómico de la Localidad Laguna Flecha Negra (Complejo Bahía Laura,
57 Jurásico Medio-Superior), Provincia de Santa Cruz, Argentina. Se reconocieron las
58 facies sedimentarias y los estilos preservacionales para definir las tafofacies en la
59 secuencia estudiada. En este trabajo se identifican once tafofacies para plantas y se
60 proponen las fuentes de aporte de material vegetal dentro de un marco geológico de
61 sistema volcánico y geotermal. Los restos corresponden a plantas autóctonas a para-
62 autóctonas, y su mejor preservación se observa en facies distales de sistemas
63 geotérmicos silíceos. Se encontraron variaciones tafonómicas laterales y verticales en la
64 secuencia estudiada. Estas diferencias se atribuyen a cambios en el aporte sedimentario
65 y a la distancia a las emanaciones geotermales. Los resultados obtenidos permiten
66 reconstruir la evolución geológica en esta región del Macizo del Deseado. Se interpreta
67 la generación de un sistema de *hot-spring* silíceo que fue destruido subsecuentemente
68 por una erupción freática en el margen de un domo andesítico en facies de flujo
69 piroclástico parcialmente retrabajado. Luego de la destrucción del sistema geotermal, se
70 desarrollaron subfacies epiclásticas fluviales y lacustres en las cuales se produjo la
71 fosilización de una comunidad vegetal jurásica. La actividad volcánica de la región dio
72 origen a subfacies piroclásticas, con potentes depósitos de caída y flujo piroclásticos
73 con distintas procedencias, y separados por un hiato temporal que promovió la
74 fosilización de un bosque *in situ*. Los estudios tafonómicos de estas comunidades
75 vegetales permitieron reconocer una serie de eventos geológicos y cómo estos procesos
76 influenciaron la preservación de una flora Jurásica de Patagonia. Con este trabajo se
77 contribuye al conocimiento de la paleoecología de la provincia geológica del Macizo del
78 Deseado.

79 **Palabras clave.** Paleobotánica. Tafonomía. Humedales geotérmicos. Depósitos
80 volcániclásticos. Reconstrucción paleoambiental. Macizo del Deseado.

81 TAPHONOMY is the science that examines the processes affecting organism remains
82 during fossilization, burial, and exhumation (Brenchley & Harper, 1998). It is a term
83 forged by Efremov (1940) to refer to the history of fossilized remains. Traditionally,
84 taphonomy includes two aspects: biostratinomy and fossil diagenesis. Biostratinomy
85 includes the sedimentological history of the organic remains, up to and including burial
86 (Gee & Gastaldo, 2005). This includes abrasion, fragmentation, dislocation,
87 reorientation and sorting, collectively a set of processes that can be recognized in the
88 fossil record (Speyer & Brett, 1988; Fernández-López & Fernández-Jalvo, 2002). Fossil
89 diagenesis includes those processes that start after the burial of an organism or a portion
90 of the organism, and which convert the organism into a fossil (e.g. compression, re-
91 crystallization, replacement) (Gee & Gastaldo, 2005). These processes lead to physical
92 and chemical balance between the plant remains and the sedimentary environment
93 (Martín-Closas & Gomez, 2004). Burial of organic remains may lead to the loss of
94 information (e.g., due to the selective preservation of different organs), but at the same
95 time, may provide additional information, since each type of fossil is indicative of the
96 depositional environment in which these remains have been accumulated, as well as
97 subsequent history. Fossilization might favor the appearance of preservational
98 modifications, which may therefore increase the available taphonomic information
99 (Fernández López, 1991). In such circumstances, the taphonomic history of organic
100 remains may be strongly correlated to the environmental conditions and sedimentary
101 environment, as reflected in various taphonomic attributes (Speyer & Brett, 1988;
102 Allison & Bottjer, 2011).

103 Taphonomic facies, or taphofacies, consist of suites of sedimentary rock
104 characterized by combinations of preservational features of the contained fossils (Brett
105 & Baird, 1986; Brett & Speyer, 1990). The concept of taphofacies describes the

106 different types of preservation found through a sedimentary succession, and the
107 different types of preservation and modes of occurrence of different fossil taxa within
108 individual horizons (Speyer & Brett, 1986; Speyer & Brett, 1988). These differences
109 allow recognition of patterns of temporal and spatial distribution of fossil remains in
110 fossil assemblages; they are the basis to integrate information about species
111 distributions and process-product associations of the fossil remains (Speyer & Brett,
112 1988). The taphonomic properties of a taphocenosis (i.e. a group of remains that were
113 buried together) are the product of specific environmental conditions (Brett & Baird,
114 1986); specifically, taphofacies are generated by an interdigitated mosaic of
115 environmental conditions. In this sense, taphofacies models describe the distributions of
116 taphonomic conditions that have a direct correspondence with environmental
117 phenomena that can be empirically determined (Speyer & Brett, 1988). In plants,
118 taphonomic studies incorporate the complexity of different organs (e.g. roots, branches,
119 leaves, seeds) behaving differently under the same environmental processes and
120 conditions (Colombi & Parrish, 2008; Bodnar, 2010), and the same organ behaving
121 differently when environmental conditions change (Bodnar, 2010). In this sense,
122 taphonomic studies of plants are a potent tool for paleoenvironmental and paleoclimatic
123 reconstructions (Bodnar, 2010).

124 The Middle-Late Jurassic Bahía Laura Complex in Santa Cruz Province, hosts
125 fossil-rich deposits formed in or at the margins of geothermal systems (Channing *et al.*,
126 2007; García Massini *et al.*, 2012a, 2016; Guido & Campbell, 2009, 2011, 2012, 2017,
127 2019; Guido *et al.*, 2010; Sagasti *et al.*, 2016, 2018, 2020). These are comparable to the
128 famous Devonian Rhynie Chert (e.g. Channing *et al.*, 2011; García Massini *et al.*,
129 2012a, 2016); however, the deposits from Bahía Laura Complex crop-out in large
130 geothermal fields that have experienced low to none post-depositional disturbance (i.e.

131 tilting, faulting). Plant fossils from the Deseado Massif paleo hot springs are distributed
132 over different geothermal sub environments, presumably following specific ecological
133 preferences (Channing *et al.*, 2007, 2011; García Massini *et al.*, 2012a, 2016; Guido *et*
134 *al.*, 2010; Sagasti *et al.*, 2016). Silicification processes affecting these environments
135 have also lead to fossilization of interactions between plants, arthropods, fungi and other
136 microorganisms (García Massini *et al.*, 2012b, 2016; Sagasti *et al.*, 2018). In this paper,
137 we provide the first description and interpretation of plant taphofacies in the Bahía
138 Laura Complex at the Laguna Flecha Negra locality, Santa Cruz Province, Patagonia,
139 Argentina. We integrate these taphofacies with depositional models for siliceous hot
140 spring deposits, or sinters, volcanic and volcanoclastics rocks, intending to reconstruct
141 the paleoenvironmental settings in which the fossil plant assemblages were preserved.

142 **Institutional abbreviations.** MPM PB, Museo Padre Jesús Molina, Paleontological
143 Collection, Santa Cruz Province, Argentina.

144 **MATERIAL AND METHODS**

145 Field methods included a detailed sedimentological logging of the outcrops taking into
146 consideration grain size, color, composition, primary sedimentary structures, and
147 geometry of the horizons, as well as contacts and vertical passage between successive
148 rock beds (Selley, 2000). During logging we identified the fossil-bearing levels
149 mentioned in an initial report of this locality (Channing *et al.*, 2007). For each fossil
150 horizon a detailed description of the fossil remains *in situ* was made (i.e. type of organs,
151 sorting, degree of fragmentation, density, and spatial distribution).

152 Sedimentary facies were defined following the criteria of Walker (1992),
153 Reading and Levell (1996), Scasso and Limarino (1997) and Miall (2006). Walker
154 (1992) defines the concept of facies as a rock body characterized by a particular
155 combination of lithology and physical and biological structures that generate an aspect

156 (=facies) that is different from the adjacent rocks. The characterization of clastic rocks
157 requires an initial identification of the lithology in terms of composition, texture,
158 sedimentary structures, the geometry of the bedding, paleocurrents and fossil content
159 (Scasso & Limarino, 1997). Detailed analysis of these features allows the definition of
160 facies present in a rock sequence, which, along with the application of Walther's Law,
161 is essential to recognize the genesis of sedimentary deposits and paleoenvironmental
162 changes through time. The analysis and interpretation of the facies association were
163 made following the criteria of Guido (2004). The sedimentological section was
164 illustrated using CorelDraw 2019, with a scale of 1:250.

165 Ten preservational styles have been defined at the Laguna Flecha Negra locality:
166 (1) individual permineralization of roots (**Rp**), (2) stem casts (**Cs**), (3) carbonized wood
167 (**Cw**), (4) massive siliceous permineralizations (**Ch**), (5) individual permineralizations
168 of stems (**Ps**), (6) impressions of leaves, leafy twigs and reproductive structures (**I**), (7)
169 impression-compressions (**IC**), (8) vertical silicified stems and stumps (**Sv**), (9)
170 horizontal to oblique silicified stems and stumps (**Sh**), and (10) compressions of plant
171 debris (**D**). Different types of fossils were classified following the criteria of
172 Archangelsky (1970), Willis and McElwain (2002) and Taylor *et al.* (2009). For the
173 definition of taphofacies, a combination of codes of letters for the preservational styles
174 and lithofacies was applied following Speyer and Brett (1986, 1988), Guido (2004),
175 Colombi and Parrish (2008) and Bodnar (2010). The attributes used are as follow:
176 sedimentary facies, types of fossils, density, and degree of fragmentation. Comparisons
177 were made with models of sedimentation in geothermal environments of the Deseado
178 Massif (Guido *et al.*, 2010; Guido & Campbell, 2011; Guido *et al.*, 2019) and with
179 modern geothermal systems (Channing & Edwards, 2013; Channing, 2017).

180 **Geological setting**

181 The Deseado Massif, Santa Cruz Province (southern Patagonia), is a geological
182 province with a 60,000 km² areal range, that is characterized by extensive Middle to
183 Late Jurassic bimodal volcanic rocks, including calc-alkaline rhyolites and minor
184 andesites and dacites (Guido & Campbell, 2011). Jurassic volcanic units recognized in
185 the province are included in the Bahía Laura Complex which encompasses: The Bahía
186 Laura Group (La Matilde and Chon Aike formations) represented by the extensive acid
187 volcanic rocks (Guido, 2004), and the andesites of the Bajo Pobre Formation; which are
188 genetically related units that appear intercalated in several localities in Santa Cruz
189 Province (Guido & Campbell, 2011). Bahía Laura volcanic rocks and related
190 hydrothermal mineralization of the Deseado Massif were formed due to extension,
191 magmatism, and a high thermal gradient from Middle to Late Jurassic (Guido &
192 Campbell, 2011). Radiometric analysis estimate that volcanism and crustal extension
193 occurred between 177.8 and 153.4 My (Féraud *et al.*, 1999; Pankhurst *et al.*, 2000).

194 Figure 1

195 Studies were conducted at the Laguna Flecha Negra locality, in a region located
196 around 69°48'W and 47°55'S, in the Deseado Massif geological province,
197 approximately 100 km NNE of Gobernador Gregores, in Santa Cruz, Argentina (Fig. 1).
198 This locality is included in the topographic chart 4669-I (Gobernador Gregores) at a
199 1:250,000 scale (Panza & Marín, 1998). The Laguna Flecha Negra locality records a
200 fossil flora contained in rhyolitic, pyroclastic and epiclastic (fluvial) deposits with chert
201 lenses located in the western edge of a 400 m diameter dry lagoon (Figs. 1.1, 2)
202 (Channing *et al.*, 2007; Sagasti, 2018; Sagasti *et al.*, 2018, 2020). The outcrop sequence
203 of Laguna Flecha Negra has been attributed to Middle-Late Jurassic Chon Aike and
204 Bajo Pobre formations based on lithological characteristics and stratigraphic
205 relationships with the units of the Bahía Laura Group (Channing *et al.*, 2007). The Bajo

206 Pobre, Chon Aike and La Matilde formations intercalate variably along Santa Cruz
207 Province, thus we prefer the use of volcanic facies within the Bahía Laura Complex
208 stratigraphic unit, as proposed by Echeveste *et al.* (2001) and Guido *et al.* (2006). Table
209 1 summarizes the facies defined for the Laguna Flecha Negra outcrops.

210

211 Table 1

212 The lowest part of the Bahía Laura Complex at Laguna Flecha Negra comprises
213 an andesitic lava dome (Ld facies at Figs. 1.1, 2). These lavas contain angular basic
214 xenoliths and evidence of hydrothermal and weathering alteration such as degraded
215 biotites and blue-green coloration. The margins of the outcrops of the lava have been
216 weathered to an orange residue.

217 Stratigraphically above this unit is an unconformity overlain by a 12.5 m thick
218 horizon of coarse, massive, white-colored volcanic sandstone (Figs. 1.1, 2.1–2, Scm
219 facies). Weathering at this stratigraphic level is evidenced by an orange-mottled surface.
220 The sandstone comprises angular volcanic lithic clasts and eroded feldspar crystals. The
221 sandstone level contains fossil plants preserved as impressions, casts, compressions,
222 small carbon pieces and permineralizations. Two chert lenses (Figs. 1.1, 2.2, facies Ch),
223 of 20 cm thickness each, are contained within the sandstone.

224 Figure 2

225 Conformably overlying the white sandstone is five meters of interbedded fine
226 sandstone and dark siltstone (Figs. 1.1, 2.3, facies SfSc). Bed thicknesses increase
227 upwards to 10-35 cm, each with upward-fining sand to silt internal structure. These beds
228 are initially cross-bedded and then transition upwards to parallel bedding. Bedding
229 surfaces contain heavily weathered volcanic clasts, ash particles and mica flakes. A
230 well-preserved flora was collected from SfSc facies (Sagasti *et al.*, 2020).

231 Conformably overlying the dark siltstone and sandstone beds are 15 meters of
232 massive white tuffs, which have been identified as volcanic ash fall deposits named
233 Tobas de Caída El Fénix unit by Echeveste *et al.* (2001) and Channing *et al.* (2007).
234 The tuffs fine upward from coarse to fine, with lapilli-rich horizons at the top. The
235 uppermost part of this stratigraphic section constitutes an *in situ* permineralized forest
236 that extends for about 1 km on a paleo-slope, and contains sparse twig impressions
237 embedded within the tuffaceous sediments (Figs. 1.1,2.4, Tm facies).

238 The fossiliferous strata are covered to the north and west by a 12.5-meter-thick,
239 pink rhyolitic ignimbrite lying unconformably over the volcanoclastic sediments (Figs.
240 1.1,2, facies Ir). This corresponds to the Ignimbrita Flecha Negra unit of Echeveste *et*
241 *al.* (2001) and represents the youngest member of the Bahía Laura volcanic Complex in
242 this locality.

243 **RESULTS**

244 **Taphofacies**

245 Eleven taphofacies were identified at the Laguna Flecha Negra locality: (1) white coarse
246 sandstone with individual permineralized roots [**Scm(Rp)**]; (2) white coarse sandstone
247 with stem casts [**Scm(Cs)**]; (3) white coarse sandstone with carbonized wood
248 [**Scm(Cw)**]; (4) chert lenses with plant fragments [**Ch(Ch)**]; (5) white coarse sandstone
249 with individual permineralized stems [**Scm(Ps)**]; (6) white coarse sandstone with
250 impressions of leaves, leafy twigs and reproductive structures [**Scm(I)**]; (7) fine
251 sandstone and cross-laminated siltstone with impressions-compressions of leaves, leafy
252 twigs and reproductive structures [**SfSc(IC)**]; (8) fine sandstone and cross-laminated
253 siltstone with impressions-compressions of plant debris [**SfSc(D)**]; (9) massive tuffs
254 with vertical permineralized stems and stumps [**Tm(Sv)**]; (10) massive tuffs with
255 horizontal and oblique permineralized stems and stumps [**Tm(Sh)**]; (11) massive tuffs

256 with imprints and casts of small branches [**Tm(I)**]. Taphofacies 1 to 6 are found in
257 stratigraphic horizon 2, taphofacies 7 and 8 in stratigraphic horizon 3, and taphofacies 9
258 to 11 in stratigraphic horizon 4 (Fig. 2).

259 *Taphofacies Scm(Rp)*. This taphofacies consists of tabular bodies of massive,
260 white colored, coarse sandstone with evidence of subaerial exposure above an orange
261 mottled surface, and characterized by the presence of preservational style Rp (Figs. 3.1–
262 2), which comprises individual permineralized roots. Individual roots are, non-ramified
263 fragments that range from 0.5 to 3 cm diameter and are up to 60 cm long that have
264 undergone silicic permineralization. Roots are set perpendicular, oblique, or parallel to
265 the stratification surface; occur in small groupings and have a somewhat clumped
266 distribution within host sediments.

267 Figure 3

268 *Taphofacies Scm(Cs)*. This taphofacies constitutes tabular bodies of massive,
269 white colored, coarse sandstone with an orange mottled surface. It is characterized by
270 the presence of preservational style Cs: stem casts (Fig. 3.3). Casts are three-
271 dimensional, 30 cm long, 10 cm wide, and have a striated surface which usually appears
272 to be superficially oxidized. Casts are positioned almost parallel to the stratification
273 surface and close to the occurrence of carbonized wood material (Cw, below).

274 *Taphofacies Scm(Cw)*. This taphofacies consists of tabular bodies of massive,
275 white colored, coarse sandstone with an orange mottled surface, and is characterized by
276 the presence of preservational style Cw: fragments of carbonized wood (Fig. 3.4).
277 Charcoalified wood fragments are small, with a maximum size of 10 cm long and 15 cm
278 wide. Wood fragments appear in small groupings, randomly distributed, and parallel to
279 the stratification surface.

280 *Taphofacies Ch(Ch)*. This taphofacies comprises two lenticular chert levels (Fig.
281 3.5–6), of up to 20 cm thick and 3 meters of outcrop length, contained within white
282 coarse sandstone in the northwestern part of the Laguna Flecha Negra locality. The
283 siliceous matrix contains abundant plant remains of variable sizes, many of which are
284 preserved parallel to the stratification surface (Fig. 3.5). Some fragments display good
285 anatomical detail and almost intact morphologies (Fig. 3.6).

286 *Taphofacies Scm(Ps)*. This taphofacies is typified by tabular bodies of massive,
287 white colored, coarse sandstone with siliceous cement and an orange mottled surface.
288 Plant fossils comprise permineralized plant axes of preservational style Ps (Fig. 3.7).
289 Fragments of silicified plant axes range from 4.4 cm to 11.7 cm in diameter and from
290 2.2 to 6.7 cm long. These occur in high concentrations, always parallel to the
291 stratification surface. Preservation is good to poor, allowing anatomical studies (Sagasti,
292 2018).

293 *Taphofacies Scm(I)*. This taphofacies constitutes tabular bodies of massive,
294 white colored, coarse sandstone with an orange mottled surface. The rocks are strongly
295 cemented with silica. Plant fossils are characterized by preservational style I,
296 impressions of leaves, leafy twigs and reproductive structures (Fig. 3.8) with variable
297 degrees of fragmentation, and with some displaying oxidized surfaces. Fossils occur
298 parallel to the stratification surface within the plant-bearing levels. Plant organs are
299 widely distributed in the sediments and can be extracted as individual units.

300 *Taphofacies SfSc(IC)*. This taphofacies consists of tabular bodies of fine
301 sandstone and dark siltstone. Rock beds fine upwards from fine sandstone to siltstone.
302 Beds are cross-laminated at the base and shift to parallel laminated towards the top (Fig.
303 2). Volcanic lithics appear strongly weathered over the stratification surface, occurring
304 with ash particles and mica flakes. Plant fossils are characterized by preservational style

305 IC, impressions-compressions (Fig. 3.9). This preservational style comprises leaves,
306 leafy twigs and reproductive structures in the form of an amorphous carbonaceous film
307 that does not preserve anatomical features and has no associated cuticles. Fossils are
308 abundant within the plant-bearing level and occur parallel to the stratification surface.
309 There is no significant superimposition of organs, allowing the isolated extraction of
310 samples.

311 *Taphofacies SfSc(D)*. This taphofacies constitutes tabular bodies of fine
312 sandstone and dark siltstone. The rocks fine upwards from fine sandstone to siltstone,
313 are cross-laminated at the base, and parallel laminated towards the top. Volcanic lithics
314 are strongly weathered on bedding planes and co-occur with ash particles and mica
315 flakes. Plant fossils are characterized by preservational style D: plant debris (Fig. 3.12).
316 This preservational style consists of finely comminuted and compressed, individually
317 unidentifiable plant fragments in layers set parallel to the bedding plane.

318 *Taphofacies Tm(Sv)*. This taphofacies comprises tabular bodies of white tuff,
319 fining upwards from coarse to fine grain sizes, with thin horizons of lapilli; it is
320 characterized by the presence of preservational style Sv: vertical stems and stumps (Fig.
321 3.10). Stumps are attached at the base to their roots contained in the rock. The diameters
322 of stems and stumps range from 50 cm to 1.5 meters. Stems and stumps are silicified,
323 occur perpendicular to slightly oblique to the stratification surface and in moderate to
324 high concentrations.

325 *Taphofacies Tm(Sh)*. This taphofacies is made up of tabular bodies of white tuff,
326 fining upwards from coarse to fine grain sizes, with thin horizons of lapilli. It is typified
327 by the presence of preservational style Sh, horizontal stems and stumps (Fig. 3.11).
328 Fallen trees are preserved attached to their respective bases (Fig. 3.11). Diameters of

329 trees range from 0.3 m to 1.5 m and are up to 2 meters long. Stems and stumps are
330 silicified and appear in high concentrations, parallel to the stratification surface.

331 *Taphofacies Tm(I)*. This taphofacies comprises tabular bodies of white tuff,
332 fining upwards from coarse to fine grain sizes, with thin horizons of lapilli. It is
333 characterized by the presence of preservational style I, impressions. Impressions of
334 fragments of twigs that are oriented parallel to the stratification surface.

335 **Spatial distribution of taphofacies**

336 The sequence studied at Laguna Flecha Negra preserves effusive lavas and
337 volcanoclastic rocks of the Bahía Laura Complex. Figure 1.1–2 shows the spatial
338 distribution of litho- and taphofacies at the Laguna Flecha Negra locality. Close to the
339 lagoon edge, the sandstone contains taphofacies Scm(Rp), Scm(Cs), Scm(Cw), Ch(Ch),
340 Scm(Ps), and in minor abundance, Scm(I). In the southern part of the locality there is a
341 greater representation of taphofacies Scm(I), whilst taphofacies Scm(Rp), Scm(Cs),
342 Scm(Cw), Scm (Ps) and Ch(Ch) are absent. Taphofacies SfSc(IC) and SfSc(D) are
343 distributed along the cliffs that bound this sequence. The sandstone and siltstone unit is
344 overlain by massive tuffs, which lack fossils in most of their vertical distribution, except
345 for at the top of the sequence, which hosts taphofacies Tm(Sv), Tm(Sh) and Tm(I). The
346 volcanoclastic sequence ends with the Ignimbrita Flecha Negra, a lithofacies that does
347 not preserve any type of fossil.

348 **DISCUSSION**

349 **Incorporation pathways for plant material**

350 The study of modern terrestrial geothermal systems with subaerial siliceous
351 thermal spring-aprons and geothermally influenced wetlands allow division into three
352 general areas along a discharge gradient: proximal near-vent, with high temperatures
353 (>59°C); mid-slope apron, with a moderate temperature (~59° to 35° C); and distal

354 slope apron, with low temperatures (<35°C) (Fig. 4.1 inset) (*e.g.*, Walter, 1976; Cady &
355 Farmer, 1996; Channing *et al.*, 2004). Fluid composition and mineralization processes
356 along these gradients generate recurring biological and textural associations that allow
357 comparisons with fossil systems (Guido & Campbell, 2011).

358 There are three main paths for the incorporation of plant material in modern hot-
359 spring systems (Channing & Edwards, 2013): (1) allochthonous and para-autochthonous
360 organs that fall from the local vegetation, both within the hot spring system, and at its
361 margins, (2) autochthonous communities that are fossilized by progradation of aprons
362 and geothermal wetland margins, and (3) herbaceous communities that replace arboreal
363 components after long periods of flooding, and which are permineralized in life
364 position. In Laguna Flecha Negra, taxonomical analyses of the taphocenosis have
365 shown that paleocommunities were dominated by microphyllous conifers of the families
366 Araucariaceae, Cheirolepidiaceae, Cupressaceae (*s.l.*) and Podocarpaceae, as well as
367 leafy branches with no definite familiar affinities (Sagasti, 2018; Sagasti *et al.*, 2020).
368 Cycadeoids were also abundant, whilst ferns and possible pteridosperms had lower
369 diversity and abundance (Sagasti, 2018; Sagasti *et al.*, 2020). Horizontal distribution of
370 different organs is consistent with preservational biases that affect fossilization
371 processes of plant parts. Woody organs are concentrated in sediments with high porosity
372 and influence of mineral-rich fluids, whilst laminar organs and reproductive structures
373 become preserved as impressions and compressions in rocks with lower porosity and
374 without geothermal influence.

375 Within the chert lenses of Laguna Flecha Negra, there are abundant plant
376 remains showing variable degrees of fragmentation. Gymnospermous leafy twigs with
377 anatomical details, fern petioles, fragmented pinnulae, roots, and leaves with multiple
378 vascular bundles are preserved. Studies of silicified fossil plants from geothermal

379 settings are abundant, most frequently addressing plants of the Rhynie chert (*e.g.*,
380 Channing, 2001, 2003; Channing & Edwards, 2009 a, b; Edwards & Selden, 1993;
381 Edwards *et al.*, 1998; Kenrick & Crane, 1997; Taylor & Berbee, 2006; Trewin, 2001).
382 These show how preservation status varies according to environmental conditions and
383 speed of silicification. Plants growing in the most humid habitats of Rhynie, are usually
384 the best-preserved, whilst others that grew on better-drained substrates have their soft
385 tissues decayed or missing (Kerp, 2018). Plants preserved within the cherts of Laguna
386 Flecha Negra present various states of decay, some preserving soft parenchymatous
387 tissues whilst others are only fragments of woody material. This disparity in decay
388 states and the abundance of plant material that appears randomly to parallel to
389 stratification oriented suggest that these fossils correspond to plant litter and fragments
390 that were rapidly silicified by hydrothermal fluids . Preservation of cellular detail is
391 consistent with low temperature fluids (*e.g.*, Channing & Edwards, 2009a, b, 2013,
392 Channing, 2017), which supports the interpretation of silica gel-dominant, distal sinter
393 facies affected by fluvial deposits that concentrated the transported vegetal material.

394 In the coarse sandstone horizon that contains the chert lenses in the northwestern
395 part of the study area, fossil remains of unknown affinity correspond to stems preserved
396 as casts, impressions and charcoal. In this same region, *in situ* permineralized roots, and
397 gymnosperms stems and branches occur in close proximity to each other. The presence
398 of angular volcanic lithics is indicative of a volcanoclastic source for these sediments.
399 Weathered feldspar crystals indicate a proximal source and scarce transport for these
400 sediments, that would have derivate from the underlying Bajo Pobre lava dome
401 (Channing *et al.*, 2007). Geothermal activity associated with this volcanic event would
402 have favored the development of mineral rich fluids that flowed following the

403 topography to generate the chert lenses found at the margin of the Laguna Flecha Negra
404 lagoon.

405 The absence of chert lenses in the rest of the locality also contributes to the
406 interpretation of chert lenses as distal facies within a localized geothermal system. In
407 this area, sandstones have a higher content of silica cement, contain a well-preserved
408 flora of impressions, and have no evidence of geothermal influence. Overlying these
409 sandstones, the sequence is volcanoclastic in origin. In the southwestern area of the
410 locality the association of taphofacies SfSc(IC) and SfSc(D) occurs in horizons that
411 range from 10 to 35 cm thickness. This is the thinnest level of the sequence, and points
412 to a later reworked stage of the volcanic event. It is also the clastic level with the
413 greatest abundance of organic material. Horizons preserve both, an autochthonous and
414 para-autochthonous flora that shows well-preserved organs and abundant plant debris.
415 Presence of cross- to parallel lamination, plant debris, and texture of the rocks could
416 indicate a fluvial to lacustrine origin.

417 Depositional environments determine the accuracy with which a fossil
418 community reflects the composition and structure of the original vegetation (DiMichele
419 & Falcon-Lang, 2011). In subaqueous settings, and under reducing conditions,
420 decomposers activity is limited and, thus, plant material is slow to decay, whereas, in
421 superficial and oxygenated environments, organic decay occurs rapidly (Trewin &
422 Fayers, 2016). Volcanic ash-falls can bury and preserve *in situ* vegetation almost
423 instantly, allowing preservation of horizontal structure of plant communities over a vast
424 area around a volcanic building (Johnson, 2007; DiMichele & Falcon-Lang, 2011).
425 Taphocenosis preserved in the same spatial conformation as in life, and which have
426 undergone little or no biostratigraphic filtering following plant death, are called “T₀
427 assemblages” (DiMichele & Gastaldo, 2008; DiMichele & Falcon-Lang, 2011;

428 Channing & Edwards, 2013). The rate of accumulation of sediment plays a major role in
429 the preservation of a T₀ assemblage (DiMichele & Falcon-Lang, 2011). Landscapes
430 buried faster preserve the vegetation structure with greater fidelity (Johnson, 2007).
431 Fossil forests such as the one preserved in Laguna Flecha Negra are an example of T₀
432 assemblage since it preserves *in situ* stems and stumps that were covered by ash-fall
433 deposits. These type of fossil assemblages allow studies of paleoecological parameters
434 such as forest layers, density and age structure (*e.g.*, DiMichele *et al.*, 2006, 2007, 2009;
435 Opluštil *et al.*, 2009; Sagasti, 2018). Permineralization of erect trees has been recorded
436 mostly in dryland settings (Mencel *et al.*, 2009), in regions with abundant volcanic
437 sediment input (Matysová *et al.*, 2010), and in regions with carbonate or silica
438 availability (*e.g.*, Ballhaus *et al.*, 2012; Dawson, 1877; DiMichele & Falcon-Lang,
439 2011; Liesegang & Gee, 2020; Walton, 1935; Wnuk & Pfefferkorn, 1984). Different
440 kinds of anatomy of the entombed trees have different preservational potentials and are
441 most likely to appear in distinct physical environmental settings (DiMichele & Falcon-
442 Lang, 2011). In addition, fossil forests are likely to represent only a fragment of the
443 ecological community (Falcon-Lang *et al.*, 2009). This is evidenced at Laguna Flecha
444 Negra by the limited amount of impressions associated with the *in situ* forest.
445 Permineralized stems and stumps appear in taphofacies Tm(Sv) and Tm(Sh), closely
446 related to impressions of unidentifiable plant fragments of taphofacies Tm(I). Facies Tm
447 of the outcropping sequence of Laguna Flecha Negra preserves only the arboreal
448 component of the plant community, whilst herbaceous understory is absent, which
449 suggest the rapid burial by the Ir ignimbrite facies.

450 **Depositional history of the Jurassic Laguna Flecha Negra locality**

451 Laguna Flecha Negra provides an opportunity to assess the impact of depositional and
452 post-depositional history on fossil plant assemblages affected by volcanism and

453 geothermal activity in the geological record. The evolutionary history of this locality
454 may be reconstructed (Fig. 4) because of the structurally undisturbed nature of Jurassic
455 deposits in this region (Guido & Campbell, 2011). The detailed taphonomic and genetic
456 study described herein indicate spatial and topographic relationships amongst
457 preservational styles, source of siliceous-rich fluids and volcanic and volcanoclastic
458 input.

459 Guido (2004) analyzed the Bahía Laura Complex sequences and studied the
460 lithofacies subdivisions of the Jurassic volcanic and volcanoclastic deposits from the
461 Deseado Massif. In that work, two facies were defined (volcanoclastic and effusive) and
462 several subfacies within them. The volcanoclastic facies comprise all the fragmentary
463 volcanic deposits and include both pyroclastic and reworked volcanic rocks. Pyroclastic
464 rocks formed by explosive processes and were grouped in three subfacies: flow, fall and
465 surge deposits. The reworked volcanoclastic rocks are included in the subfacies
466 epiclastic; they appear interstratified, which prevents recognizing divisions within them
467 (Guido, 2004).

468 The effusive facies includes coherent, non-fragmented rocks, which were
469 formed by cooling and solidification of magma, without the involvement of explosive
470 events (Guido, 2004). Two subfacies can be recognized within the effusive facies:
471 extrusive lava rocks that form flows and domes (grouped in the lava subfacies), and
472 hypabyssal rocks that were consolidated in the subsurface (grouped in the sub-volcanic
473 subfacies).

474 Facies defined for the outcrops at Laguna Flecha Negra can be analyzed within
475 the context of depositional models for the Bahía Laura Complex (Table 2). Facies Ld is
476 interpreted as an effusive deposit of the lava subfacies. These andesitic domes represent
477 a late stage of volcanism and have their source to the east of the Laguna Flecha Negra

478 lagoon (Echeveste *et al.*, 2001; Channing *et al.*, 2007). These effusive andesitic deposits
479 were covered by proximal ash fall volcanic and fluvial reworked volcanoclastic deposit
480 present at Scm facies. This lithofacies also preserved, but only proximal to the Laguna
481 Flecha Negra lagoon, plant-rich chert horizons representing distal siliceous hot spring
482 facies (Figs 1;2).

483 Table 2

484 Channing *et al.* (2007) identified the presence of cross-cutting NW-SE striking
485 chalcedony veining with minor carbonate mineralization to the north-western edge of
486 the Laguna Flecha Negra lagoon. Stratigraphic relationship between veining and chert
487 beds was not established although they shared mineral composition and trace elements
488 (Channing *et al.*, 2007). We hypothesize the presence of surface geothermal springs
489 forming sinter close to the NW oriented fault containing the chalcedony veins. The
490 spring drainage would have followed the paleoslope preserving vegetal debris in its way
491 and driving extensive permineralization. The influence of these geothermal fluid flow
492 would have promoted the preservation of roots and conifer axes as loci of
493 permineralization that occur in the coarse sandstones (facies Scm) and which contain
494 the chert lenses of the sequence.

495 Ld and Scm and Ch facies were interpreted as formed almost simultaneously,
496 with not preserved hot-spring sinter terrace deposits forming at the edge of the
497 hydrothermally altered andesitic domes, close or at the actual location of the Laguna
498 Flecha Negra lagoon (Fig. 4.1).

499 Fig. 4.2 shows an interpretation for the lack of the sinter apron as a result of
500 hydrothermal eruption breccia event in the lagoon whose crater area is covered by
501 modern sediments. A fluvial and lacustrine setting was established after the eruption,
502 which is evidenced by sedimentary structures of facies SfSc (i.e. parallel to cross-

503 bedding, finning upwards), as well as preservational styles observed (i.e. impression-
504 compressions of leaves and compressions of plant debris).

505 Figure 4

506 Facies Ch and SfSc can be correlated to the epiclastic subfacies as they are
507 composed of volcanoclastic and vegetal debris transported by water, as is indicated by
508 their sedimentary structures.

509 Facies Tm correspond to an explosive stage of the Middle-Late Jurassic
510 volcanism from the Bahía Laura Complex. It can be assigned to a fall pyroclastic
511 subfacies and is related to the volcanic center proposed by Echeveste *et al.*, (2001),
512 located to the west of this locality. This explosive fall stage was so intense that it did not
513 preserve plants but the hiatus in volcanic activity after this eruption favored the
514 development of a forest at the top of the sequence (Fig. 4.3).

515 The extraordinary preservation of the *in situ* forest is explained by the rapid
516 burial produced by Ir pyroclastic flow subfacies (Fig. 4.4), named Ignimbrita Flecha
517 Negra by Echeveste *et al.* (1999). Direction of emplacement and thinning of the
518 ignimbrite suggests a vent to the North.

519 **Geothermal environments of the Deseado Massif**

520 To date, 23 paleo-hot spring sites are known for the Deseado Massif. Five of these were
521 studied in detail to generate sedimentary models, namely San Agustín, Cerro Negro, El
522 Macanudo, La Marciana and Claudia (Guido & Campbell, 2011). Cerro Negro and El
523 Macanudo correspond to calcareous sinters or travertines and, thus, present a different set of
524 facies than those formed in siliceous sinters (Guido & Campbell, 2011, 2012, 2017). At La
525 Marciana, proximal facies of a siliceous sinter are preserved (Guido & Campbell, 2009). Apron
526 sinter facies have poorly preserved plant stems; however, this locality has not yielded much
527 information about plant communities (Channing *et al.*, 2007; Guido & Campbell, 2009).

528 The San Agustín siliceous sinter is characterized by subaqueous spring vent mounds,
529 subaerial sinter aprons including some with deep pools, and geothermal wetlands with cooler
530 margins (Guido *et al.*, 2010). Of the hot spring-related sedimentary facies recognized at San
531 Agustín, some were inferred as formed in perennially wet conditions, whilst others presented
532 evidence of intermittent wet and dry conditions (Guido *et al.*, 2010). This locality presents a
533 complete geothermal landscape in which plants, fungi and animals are fossilized (Guido *et al.*,
534 2010; Channing *et al.*, 2011; Garcia Massini *et al.*, 2012a). The paleo-lake at San Agustín
535 accumulated large volumes of volcanic materials, as well as geothermal inputs; and offshore
536 facies in which clastic sediments preserved compression fossils of plant fragments (Guido *et al.*,
537 2010). Plant communities preserved at the margins of the hot spring system of San Agustín
538 show a high affinity with those of Laguna Flecha Negra (Sagasti *et al.*, 2020).

539 The Claudia hot spring system shows stratigraphic intercalation of sinter and
540 travertine/silicified travertine deposits, and contains all the paleoenvironmental gradients from
541 high temperature vent conduits to low temperature plant-rich facies (Guido & Campbell, 2014).
542 Studies carried out at Claudia thus far have concentrated on sedimentary facies, biological
543 signatures and depositional models (Guido & Campbell, 2011, 2014, 2019). In this geothermal
544 field, fluvial sediments containing silicified tree trunks and lacustrine deposits have been
545 recognized, but no paleontological study has been conducted yet. Permineralized plant remains
546 are observed in plant rich chert from apron margins intercalated with fluvio-lacustrine strata
547 (Guido & Campbell, 2014) that show the presence of wood fragments, young stems and
548 seedlings of probable conifers (Sagasti, pers. obs.).

549 Jurassic volcanic rocks at La Bajada locality show a typical association between
550 geothermal features, volcanoclastic fluvial or lacustrine reworked deposits and lava domes
551 (García Massini *et al.*, 2016). This locality was not part of the facies analysis carried by Guido
552 & Campbell (2011), but its geology and paleontology has been preliminary analyzed (García
553 Massini *et al.*, 2016; Nunes *et al.*, 2020). At La Bajada, a series of lineament occur, between
554 which The Valentina breccia appear as a structurally controlled, phreatic breccia pipe that has
555 been suggested as responsible for the destruction of the sinter terraces of the geothermal system

556 (García Massini *et al.*, 2016). La Bajada locality is probably the best analog to Laguna Flecha
557 Negra between the known geothermal localities of the Deseado Massif.

558 **CONCLUSIONS**

559 The analysis of taphofacies carried out at Laguna Flecha Negra contributes to the
560 interpretation of the evolutionary history of this sector of the Deseado Massif.
561 Preservational styles Ps and Ch show the greater anatomical detail between the fossil
562 remains studied at Laguna Flecha Negra. This is consistent with the presence of a
563 siliceous hot-spring in this region. Presence of silicified roots is indicative of the
564 formation of paleosoils and the establishment of a plant community. Progradation of
565 aprons at the margins of geothermal wetlands promoted the fossilization of well-
566 preserved stems and trunks (preservational style Ps), vegetal debris and branches
567 (within preservational style Ch).

568 The absence of proximal sedimentary textures of hot-spring systems can be
569 explained by a hydrothermal eruption breccia event that resulted in the absence of vent
570 and apron features. The development of subsequent local fluvial and lacustrine facies is
571 consistent with this interpretation since it is common the development of lagoons in
572 craters produced by phreatic eruption.

573 Preservational styles Scm(I), SfSc(IC) and SfSc(D) are characterized by
574 moderate to high loss of biological data through taphonomic loss. Fine sediments tend
575 to preserve morphological characters with greater detail than coarser deposits. This is a
576 feature normally observed in fossil fluvial and lacustrine settings. After this epiclastic
577 event, a thick and rapid volcanic ash-fall event covered the landscape generating facies
578 Tm with no plant preservation. On top of this ash deposit, a conifer forest was
579 established and later entombed by the Ignimbrita Flecha Negra.. It is interesting to note
580 that although silica-rich fluids promoted the fossilization of stems and stumps, high

581 temperatures associated to the pyroclastic flow led to cellular deformation and poor
582 anatomic detail observed in fossils from taphofacies Tm(Sv) and Tm(Sh).

583 Taphonomic studies allow recognition of mechanisms that operate in the
584 incorporation of plant remains to the fossil record. As mentioned, sedimentary input
585 plays a fundamental role in the preservational potential of different organs. In this sense,
586 volcanoclastic environments, especially those with the presence of geothermal fluids,
587 constitute propitious settings for the preservation of plants in their different modes.
588 Combining geologic, sedimentologic and taphonomic studies allows an integrated
589 reconstruction of the sedimentary paleoenvironment and its relationship with the biota
590 that inhabited it. In this way, more holistic reconstructions can be made and thus a better
591 understanding of dynamics operating in sedimentary basins from the past is achieved.

592 **ACKNOWLEDGMENTS**

593 We thank the Culture Bureau of Santa Cruz Province for supporting our research and
594 granting us the research permits to study the Bahía Laura Complex deposits in the
595 Deseado Massif. Partial funding for this project comes from UNLP (Proy. Inc. N/807),
596 PICT 2014-3496 (JGM and DG), PIP 2011-2013 (JGM) and the National Geographic
597 Society. The paper benefited greatly from the constructive comments and suggestions of
598 Scientific Editor of Ameghiniana Dr. Adriana Mancuso, as well as two referees.

599 **REFERENCES**

- 600 Allison, P. A., & Bottjer, D. J. (2011). *Taphonomy: Process and Bias Through Time*.
601 Second edition. (612 pp) Springer.
- 602 Archangelsky, S. (1970). *Fundamentos de Paleobotánica*. Facultad de Ciencias
603 Naturales y Museo, Universidad Nacional de la Plata, Serie técnica y Didáctica
604 10, 347 pp.

605 Ballhaus, C., Gee, C. T., Bockrath, C., Greef, K., Mansfeldt, T., & Rhede, D. (2012).
606 The silicification of trees in volcanic ash—an experimental study. *Geochimica et*
607 *Cosmochimica Acta*, 84, 62–74.

608 Bodnar, J. (2010). *La paleoflora triásica de la Formación Cortaderita en la quebrada*
609 *homónima, Cuenca de Barreal-Calingasta, Provincia de San Juan, Argentina*.
610 Unpublished Thesis. 291 pp.

611 Brenchley, P. J., & Harper, D. A. T. (1998). *Palaeoecology: Ecosystems, environments*
612 *and evolution*. Chapman and Hall. London, United Kingdom. 407pp.

613 Brett, C. E., & Baird, G. C. (1986). Comparative taphonomy: a key to
614 paleoenvironmental interpretation based on fossil preservation. *Palaios* 1, 207–
615 227.

616 Brett, C. E., & Speyer, S. E. (1990). Taphofacies. In: Briggs, D. E. G., & Crowther, P.
617 R. (Eds.). *Palaeobiology: a synthesis* (pp. 258–262) Blackwell Science.

618 Cady, S. L., & Farmer, J. D. (1996). Fossilization processes in siliceous thermal springs:
619 trends in preservation along thermal gradients. In *Ciba Foundation Symposium*.
620 (pp. 150–173) John Wiley and Sons Ltd.

621 Channing, A. (2001). *Processes and environments of vascular plant silicification*.
622 Unpublished Doctoral Thesis. Cardiff University (United Kingdom) 352pp.

623 Channing, A. (2003). The Rhynie chert early land plants: palaeoecophysiological and
624 taphonomical analogues. *Transactions of the Institution of Mining and*
625 *Metallurgy (Section B: Applied Earth Science)* 112, 170–171.

626 Channing, A. (2017). A review of active hot-spring analogues of Rhynie: environments,
627 habitats and ecosystems. *Philosophical Transactions of the Royal Society B* 373,
628 20160490. DOI: 10.1098/rstb.2016.0490

- 629 Channing, A., & Edwards, D. (2009a). Silicification of higher plants in geothermally
630 influenced wetlands: Yellowstone as a Lower Devonian Rhynie analog. *Palaios*
631 *24*, 505–521.
- 632 Channing, A., & Edwards, D. (2009b). Yellowstone hot spring environments and the
633 palaeo-ecophysiology of Rhynie chert plants: towards a synthesis. *Plant Ecology*
634 *& Diversity 2*, 111–143. DOI: 10.1081/17550870903349359
- 635 Channing, A., & Edwards, D. (2013). Wetland megabias: ecological and
636 ecophysiological filtering dominates the fossil record of hot spring floras.
637 *Palaeontology* 1–34. doi:10.1111/pala.12043.
- 638 Channing, A., Edwards, D., & Strutevant, S. (2004). A geothermally influenced wetland
639 containing unconsolidated geochemical sediments. *Canadian Journal of Earth*
640 *Sciences. 41*, 809–827.
- 641 Channing, A., Zamuner, A. B., Edwards, D., & Guido, D. M. (2011). *Equisetum*
642 *thermale* sp. nov. (Equisetales) from the Jurassic San Agustín hot spring deposit,
643 Patagonia: anatomy, paleoecology, and inferred paleoecophysiology. *American*
644 *Journal of Botany 98*, 680–697.
- 645 Channing, A., Zamuner, A. B., & Zuñiga, A. (2007). A new Middle-Late Jurassic flora
646 and hot spring chert deposit from the Deseado Massif, Santa Cruz Province,
647 Argentina. *Geological Magazine 144*, 401–411.
- 648 Colombi, C. E., & Parrish, J. T. (2008). Late Triassic environmental evolution in
649 Southwesterns Pangea: plant taphonomy of Ischigualasto Formation. *PALAIOS*
650 *23*, 778–795.
- 651 Dawson, K. W. (1877). Note on a specimen of *Diploxylon* from the coal formation of
652 Nova Scotia. *Quarterly Journal of the Geological Society of London, 33*, 836–
653 842.

- 654 DiMichele, W. A., & Falcon-Lang, H. J. (2011). Pennsylvanian <<fossil forest>> in
655 growth position (T° assemblages): origin, taphonomic bias and palaeoecological
656 insights. *Journal of the Geological Society*, 168, 585–605.
- 657 DiMichele, W. A., Falcon-Lang, H. J., Nelson, W. J., Elrick, S., & Ames, P. R. (2007).
658 Ecological gradients within a Pennsylvanian mire forest. *Geology*, 35, 415–418.
- 659 DiMichele, W. A., & Gastaldo, R. A. (2008). Plant paleoecology in deep time. *Annals
660 of the Missouri Botanical Garden* 95, 144–198.
- 661 DiMichele, W. A., Nelson, W. J., & Elrick, S. D. (2006). Spatial patterns in the final
662 forest of a drowned peat mire, Springfield coal (Middle Pennsylvanian), Illinois
663 Basin. *Geological Society of America, Abstracts with Programs* 38, 380.
- 664 DiMichele, W. A., Nelson, W. J., Elrick, S., & Ames, P. R. (2009). Catastrophically
665 buried middle Pennsylvanian *Sigillaria* and calamitean sphenopsids from
666 Indiana, USA: What kind of vegetation was this? *Palaios*, 24, 159–166.
- 667 Echeveste, H., Fernández, R., Bellieni, G., Tessone, M., Llambías, E., Schalamuk, I.,
668 Piccirillo, E., & De Min, A. (2001). Relaciones entre las Formaciones Bajo
669 Pobre y Chon Aike (Jurásico medio a superior) en el área de Estancia El Fénix-
670 Cerro Huemul, zona centro-occidental del Macizo del Deseado, provincia de
671 Santa Cruz. *Revista de la Asociación Geológica Argentina* 56 (4), 548–558.
- 672 Echeveste, H., Fernández, R., Llambías, E., Tessone, M., Schalamuk, I., Bellieni, G.,
673 Piccirillo, E., & De Min, A. (1999). Ignimbritas tardías de alto grado en la
674 Formación Chon Aike (Jurásico), Macizo del Deseado, Santa Cruz. XIV
675 Congreso Geológico Argentino, Actas II 182–185.
- 676 Edwards, D., Kerp, H., & Hass, H. (1998). Stomata in early land plants: An anatomical
677 and ecophysiological approach. *Journal of Experimental Botany*, 49, 255–278.

678 Edwards, D., & Selden, P. A. (1993). The development of early terrestrial ecosystems.
679 *Botanical Journal of Scotland* 46, 337–366.

680 Efremov, J. A. (1940). Taphonomy: a new branch of paleontology. *Panamerican*
681 *Geology* 74, 81–93.

682 Falcon-Lang, H. J., Nelson, J., Elrick, S., Looy, C., Ames, P., & DiMichele, W. A.
683 (2009). Incised channel-fills containing conifers imply that seasonally-dry
684 vegetation dominated - Pennsylvanian tropical lowlands. *Geology* 37, 923–926.

685 Féraud, G., Alric, V., Formari, M., Bertrand, H., & Haller, M. (1999). $^{40}\text{Ar}/^{39}\text{Ar}$ dating
686 of Jurassic volcanic province of Patagonia: migrating magmatism related to
687 Gondwana break-up and subduction. *Earth Planet. Sci. Lett.* 172, 83–96.

688 Fernández López, S. (1991). Taphonomic concepts for a theoretical biochronology.
689 *Revista Española de Paleontología* 6, 37–49.

690 Fernández-López, S. R., & Fernández-Jalvo, Y. (2002). The limit between
691 biostratinomy and fossilization. In: De Renzi, Pardo Alonso, Belinchón,
692 Peñalver, Montoya, & Márquez-Aliaga (Eds.) *Current Topics on Taphonomy and*
693 *Fossilization*. Ayuntamiento de Valencia. Valencia, Spain. 27–36.

694 García Massini, J. L., Escapa, I. H., Guido, D. M., & Channing, A. (2016). First glimpse
695 of the silicified hot spring biota from a new Jurassic chert deposit in the Deseado
696 Massif, Patagonia, Argentina. *Ameghiniana* 53 (2), 205–230.

697 García Massini, J. L., Channing, A., Guido, D. M., & Zamuner, A. B. (2012a). First
698 report of fungi and fungus-like organisms from Mesozoic hot springs. *Palaios*
699 27, 55–62.

700 García Massini, J. L., Falaschi, P., & Zamuner, A. B. (2012b). Fungal-arthropod-plant
701 interactions from the Jurassic petrified forest Monumento Natural Bosques

702 Petrificados, Patagonia, Argentina. *Palaeogeography, Palaeoclimatology,*
703 *Palaeoecology*, 329–330, 37–46.

704 Gee, C. T., & Gastaldo, R. A. (2005). Sticks and mud, fruits and nuts, leaves and
705 climate: Plant taphonomy comes of age. *PALAIOS* 20, 415–417.

706 Guido, D. M. (2004). Subdivisión litofacial e interpretación del volcanismo jurásico
707 (Grupo Bahía Laura) en el este del Macizo del Deseado, provincia de Santa
708 Cruz. *Revista de la Asociación Geológica Argentina* 59 (4), 727–742.

709 Guido, D. M. & Campbell, K. A. (2009). Jurassic hot-spring activity in a fluvial setting
710 at La Marciana, Patagonia, Argentina. *Geological Magazine* 146 (4), 617–622.

711 Guido, D. M., & Campbell, K. A. (2011). Jurassic hot spring deposits of the Deseado
712 Massif (Patagonia, Argentina): characteristics and controls on regional
713 distribution. *Journal of Volcanology and Geothermal Research* 203, 35–47.

714 Guido, D. M., & Campbell, K. A. (2012). Diverse subaerial and lacustrine hot spring
715 settings of the Cerro Negro epithermal system (Jurassic, Deseado Massif),
716 Patagonia, Argentina. *Journal of Volcanology and Geothermal Research* 229–
717 230, 1–12.

718 Guido, D. M., & Campbell, K. A. (2017). Upper Jurassic travertine at El Macanudo,
719 Argentine Patagonia: a fossil geothermal field modified by hydrothermal
720 silicification and acid overprinting. *Geological Magazine*,
721 doi:10.1017/S0016756817000498

722 Guido, D. M., Campbell, K. A., Foucher, F., & Westall, F. (2019). Life is everywhere in
723 sinters: examples from Jurassic hot-spring environments of Argentine Patagonia.
724 *Geological Magazine* <https://doi.org/10.1017/S0016756819000815>

- 725 Guido, D. M., Channing, A., Campbell, K. A., & Zamuner, A. (2010). Jurassic
726 geothermal landscapes and fossil ecosystems at San Agustín, Patagonia,
727 Argentina. *Journal of the Geological Society, London* 167, 11–20.
- 728 Guido, D., Escayola, M., de Barrio, R., Schalamuk, I., & Franz, G. (2006). La
729 Formación Bajo Pobre (Jurásico) en el este del Macizo del Deseado, Patagonia:
730 vinculación con el Grupo Bahía Laura. *Revista de la Asociación Geológica*
731 *Argentina* 61 (2), 187–196.
- 732 Harper, C. J., Walker, C., Schwendemann, A., Kerp, H., & Krings, M. (2020).
733 *Archaeosporites rhyniensis* gen. et. sp. nov. (Glomeromycota,
734 Archaeosporaceae), from the Lower Devonian Rhynie chert- a fungal lineage
735 morphologically unchanged for more than 400 million years. *Annals of Botany*
736 mcaa113, DOI: 10.1093/aob/mcaa113.
- 737 Herbst, R. (1966). Revisión de la flora liásica de Piedra Pintada, provincia de Neuquén,
738 Argentina. *Revista del Museo de La Plata* 5, 27–53.
- 739 Johnson, K. R. (2007). Palaeobotany: Forest frozen in time. *Nature* 447, 786–787.
- 740 Kenrick, P., & Crane, P. R. (1997). The origin and early evolution of plants on land.
741 *Nature* 389, 33–39.
- 742 Kerp, H. (2017). Organs and tissues of Rhynie chert plants. *Philosophical Transactions*
743 *of the Royal Society B* 373, 20160495. <http://dx.doi.org/10.1098/rstb.2016.0495>
- 744 Knoll, A. H. (1985). Exceptional preservation of photosynthetic organisms in silicified
745 carbonates and silicified peats. *Philosophical Transactions of the Royal Society*
746 *of London B* 311, 111–122.
- 747 Liesegang, M. & Gee, C. T. (2020). Silica entry and accumulation in standing trees in a
748 hot-spring environment: cellular pathways, rapid pace and fossilization potential.
749 *Palaeontology* 63 (4), 651–660.

- 750 Martín-Closas, C., & Gomez, B. (2004). Taphonomie des plantes et interpretations
751 paléoécologiques. Une sinthése. *Geobios* 37, 65–88.
- 752 Matysová, P., Rössler, R., Götze, J., Leichmann, J., Forbes, G., Taylor, E. L., Sakala, J.,
753 & Grygar, T. (2010). Alluvial and volcanic pathways to silicified plant stems
754 (Upper Carboniferous–Triassic) and their taphonomic and palaeoenvironmental
755 meaning. *Palaeogeography, Palaeoclimatology, Palaeoecology* 292, 127–143.
- 756 Mencl, V., Matysová, P., & Sakala, J. (2009). Silicified woods from the Czech part of
757 the Intra Sudetic Basin (Late Pennsylvanian, Bohemian Massif, Czech
758 Republic): systematics, silicification and palaeoenvironment. *Neues Jahrbuch
759 für Geologie und Paleontologie, Abhandlungen* 252, 269–288.
- 760 Miall, A. D. (2006). *The geology of fluvial deposits. Sedimentary facies, basin analysis
761 and petroleum geology*. 4th edition. (582pp) Springer.
- 762 Nunes, C. I., García Massini, J. L., Escapa, I. H., Guido, D. M., & Campbell, K. (2020).
763 Conifer root nodules colonized by arbuscular mycorrhizal fungi in Jurassic
764 geothermal settings from Patagonia, Argentina. *International Journal of Plant
765 Sciences* 181, 196–209.
- 766 Opluštil, S., Pšenička, J., Libertín, M., Bek, J., Dašková, J., & Šimunek, Z. (2009).
767 Composition and structure of an in situ Middle Pennsylvanian peatforming plant
768 assemblage buried in volcanic ash, Radnice Basin (Czech Republic). *Palaios* 24,
769 726–746.
- 770 Pankhurst, R. J., Riley, T. R., Fanning, C. M., & Kelley, S. P. (2000). Episodic silicic
771 volcanism in Patagonia and the Antarctic Peninsula: Chronology of magmatism
772 associated with the Break-up of Gondwana. *Journal of Petrology* 45, 605–625.
- 773 Panza, J. L., & Marín, G. (1998). Hoja Geológica 4969-I Gobernador Gregores. Escala
774 1:250.000, Provincia de Santa Cruz. SEGEMAR. Boletín 211,77p

775 Reading, H. G. & Levell, B. K. (1996). Controls on the sedimentary rock record. In H.
776 G. Reading (Ed.) *Sedimentary environments: processes, facies and stratigraphy*.
777 (pp. 5–36). Blackwell Science.

778 Sagasti, A. J. (2018). *Estudio paleobotánico, paleoecológico y paleoambiental en la*
779 *localidad de Laguna Flecha Negra, Macizo del Deseado, Jurásico Superior,*
780 *Provincia de Santa Cruz, Argentina*. Unpublished Thesis. 253pp.

781 Sagasti, A. J., García Massini, J., Escapa, I. H., Guido, D. M., & Channing, A. (2016).
782 *Millerocaulis zamunerae* sp. nov. (Osmundaceae) from Jurassic, geothermally
783 influenced, wetland environments of Patagonia, Argentina. *Alcheringa: An*
784 *Australasian Journal of Palaeontology* DOI: 10.1080/03115518.2016.1210851.

785 Sagasti, A. J., García Massini, J. L., Escapa, I. H., & Guido, D. M. (2018). Multitrophic
786 interactions in a geothermal setting: Arthropod borings, actinomycetes, fungi
787 and fungal-like microorganisms in a decomposing conifer wood from the
788 Jurassic of Patagonia. *Palaeogeography, Palaeoclimatology, Palaeoecology*
789 doi:10.1016/j.palaeo.2018.09.004

790 Sagasti, A. J., García Massini, J. L., Escapa, I. H., Guido, D. M., & Morel, E. M.
791 (2020). Middle-Late Jurassic megaflora of Laguna Flecha Negra locality in
792 Santa Cruz Province, Patagonia, and floristic assemblages of the Bahía Laura
793 Complex. *Journal of South American Earth Sciences* 100.
794 <https://doi.org/10.1016/j.jsames.2020.102564>

795 Scasso, R. A., & Limarino, C. O. (1997). *Petrología y diagénesis de rocas clásticas*.
796 Asociación Argentina de Sedimentología, Publicación Especial Nro. 1. Capital
797 Federal, Argentina. 258pp.

798 Selley, R. C. (2000). *Applied sedimentology* (2nd Edition). Academic Press. London,
799 523 pp.

- 800 Speyer, S. E., & Brett, C. E. (1986). Trilobite taphonomy and Middle Devonian
801 taphofacies. *Palaios* 1, 312–327.
- 802 Speyer, S. E., & Brett, C. E. (1988). Taphofacies models for epeiric sea environments:
803 middle Paleozoic examples. *Palaeogeography, Palaeoclimatology,*
804 *Palaeoecology* 63, 225–262.
- 805 Taylor, J. W., & Berbee, M. L. (2006). Dating divergences in the fungal tree of life:
806 Review with some new analyses. *Mycologia* 98, 838–849
- 807 Taylor, T. N., Hass, H., Krings, M., Klavins, S. D., & Kerp, H. (2004). Fungi in the
808 Rhynie chert: a view from the dark side. *Transactions of the Royal Society of*
809 *Edinburgh: Earth Sciences* 94, 457–473.
- 810 Taylor, T. N., Taylor, E. L., & Krings, M. (2009). *Paleobotany, The Biology and*
811 *Evolution of Fossil Plants, Second Edition*, (pp. 1230) Academic Press.
- 812 Trewin, N. H. (2001). The Rhynie chert. In: Briggs, D.E.G., & Crowther, P. (Eds.)
813 *Palaeobiology II*. (pp. 342–346) Blackwell Science.
- 814 Trewin, N. H. & Fayers, S. R. (2016). Macro to micro aspects of the plant preservation
815 in the Early Devonian Rhynie cherts, Aberdeenshire, Scotland. *Earth and*
816 *Environmental Science Transactions of the Royal Society of Edinburgh* 106, 67–
817 80.
- 818 Trewin, N. H., & Kerp, H. (2017). The Rhynie and Windyfield cherts, Early Devonian,
819 Rhynie, Scotland. In: Fraser, N. C., & Sues, H. D. (Eds.) *Terrestrial*
820 *conservation lagerstätten. Windows into the Evolution of Life on Land*. (pp. 1–
821 38). Dunedin Academic Press.
- 822 Walker, R. G. (1992). Facies, facies models and modern stratigraphic concepts. In
823 Walker, R. G., & James, N. P. (Eds.) *Facies models, response to sea level*
824 *changes*. 1–14. Geological Association of Canada.

- 825 Walter, M. R. (1976). Hot-spring sediments in Yellowstone National Park. In: Walter,
826 W. R. (Ed.) *Stromatolites: Developments in Sedimentology*, 20. (pp. 489–498)
827 Elsevier.
- 828 Walton, J. (1935). Scottish Lower Carboniferous plants: the fossil hollow trees of Arran
829 and their branches (*Lepidophloios wunschianus* Carruthers). *Transactions of the*
830 *Royal Society, Edinburgh* 58, 313–337.
- 831 Willis, K. J., & McElwain, J. C. (2002). *The Evolution of Plants*. (378pp) Oxford
832 University Press.
- 833 Wnuk, C., & Pfefferkorn, H. W. (1984). The life habits and paleoecology of Middle
834 Pennsylvanian medullosan pteridosperms based on an *in situ* assemblage from
835 the Bernice Basin (Sullivan County, Pennsylvania, U.S.A.). *Review of*
836 *Paleobotany and Palynology* 41, 329–351.

837 **Figure captions**

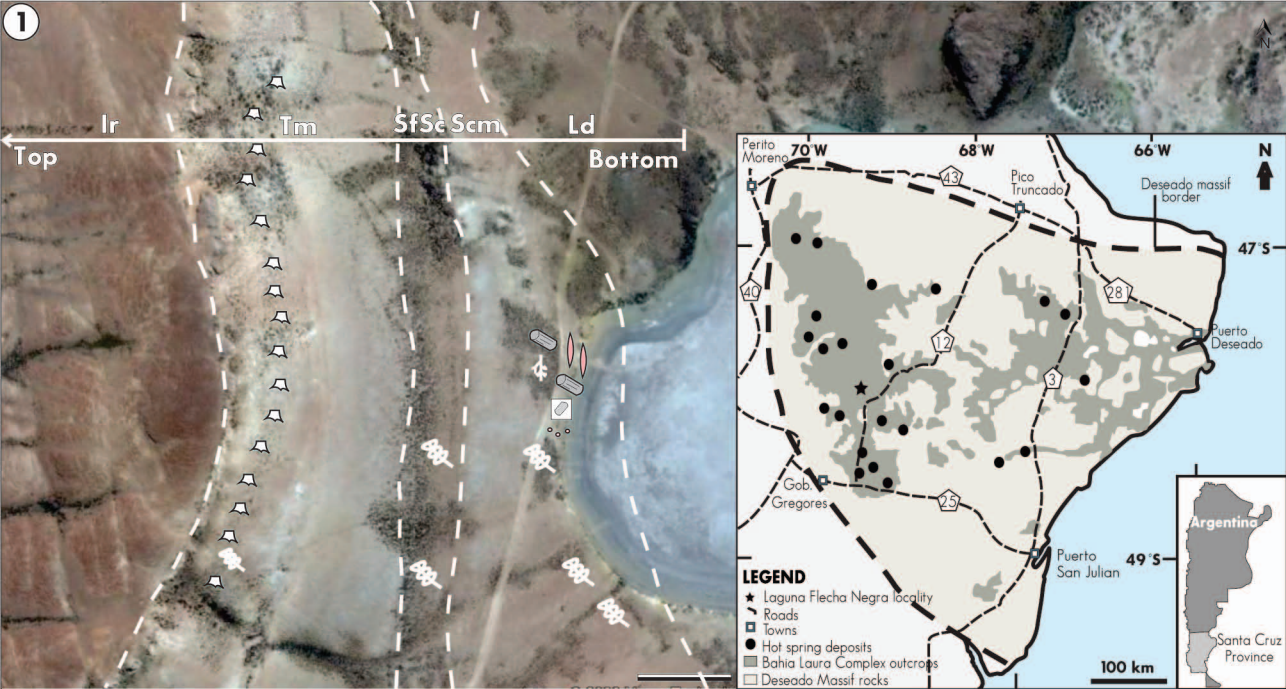
- 838 **Figure 1. 1**, Aerial view of the Laguna Flecha Negra locality showing the distribution
839 of lithofacies. Modified from Maxar Technologies2020; Google EarthPro 2020,
840 accessed January 2020. Scale: 100 m. Inset: Map of the Bahía Laura outcrops in the
841 Deseado Massif. Black dots point to geothermal localities. Laguna Flecha Negra
842 locality is marked with a black star. Modified from Sagasti *et al.* 2016. **2**, Panoramic
843 view of the Laguna Flecha Negra cliffs in which the studied succession crops-out. Areal
844 distribution of taphofacies is marked. Scale: 100 m
- 845 **Figure 2.** Stratigraphic column of the volcanoclastic succession studied at Laguna
846 Flecha Negra. Modified from Sagasti *et al.* (2018). **1**, Lithofacies Scm with
847 permineralized roots (white arrows). **2**, Lithofacies Scm and Ch. **3**, Lithofacies SfSc. **4**,
848 Lithofacies Tm.

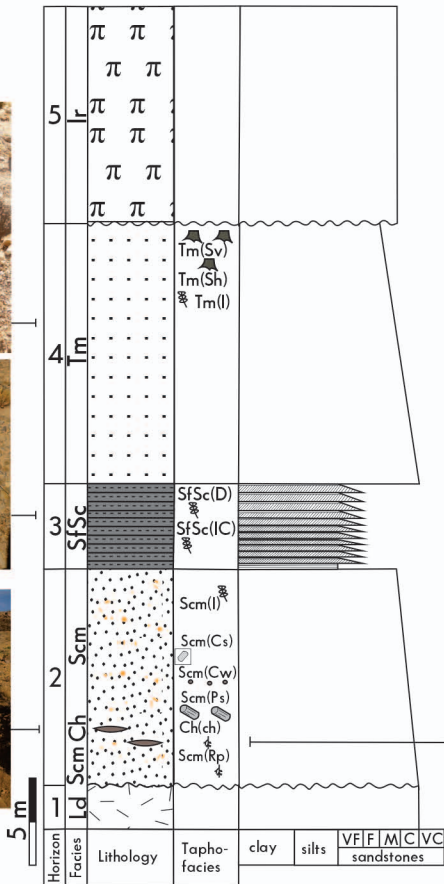
849 **Figure 3.** Preservational styles recognized in the Bahía Laura Complex at Laguna
850 Flecha Negra locality. **1**, Individual permineralization of roots in coarse sandstone.
851 MPM PB 15896. Scale: 2 cm **2**, Transverse section of permineralization of individual
852 roots in coarse sandstone. Scale: 2cm **3**, Stem casts in white tuffs. MPM PB 16028.
853 Scale: 4 cm. **4**, Carbonized wood in coarse sandstone. MPM PB 15898. Scale: 1 cm. **5**,
854 Massive siliceous permineralization (=cherts). Scale: 15 cm. **6**, Fragments of plants
855 found in the chert levels. Scale: 2 cm. **7**, Individual permineralization of stems in coarse
856 sandstone. Scale: 15 cm. **8**, Impressions of leaves in coarse sandstone. Leafy twigs and
857 reproductive structures also occur preserved as impressions. *Scleropteris vincei* Herbst
858 (1966). MPM PB 16008. Scale: 0.1 cm. **9**, Impressions-compressions of recognizable
859 plant organs in laminated silts. *Sphenopteris* cf. *nordenskiöldii*. MPM PB 15886.
860 Scale: 0.5 cm. **10**, Vertical silicified stems and stumps in massive tuffs. Stem 056.
861 Scale: 20 cm. **11**, Horizontal to oblique silicified stems and stumps in massive tuffs.
862 Stem 003. Scale 30 cm. **12**, Compressions of plant debris in laminated silts. MPM PB
863 15894. Scale: 1 cm.

864 **Figure 4. 1–4**, Schematic W–E cross-section along Laguna Flecha Negra locality
865 outcrops and their evolution during Middle–Late Jurassic. Details in text.

866 **Table 1.** Facies code for the outcrops of Laguna Flecha Negra locality.

867 **Table 2.** Lithofacies subdivision of the acid Jurassic volcanism of the Deseado Massif.
868 Modified from Guido (2004).





Legend

Sedimentary structures

- Massive
- Cross lamination
- Flat lamination
- Chert lenses
- Surface oxidized and mottled

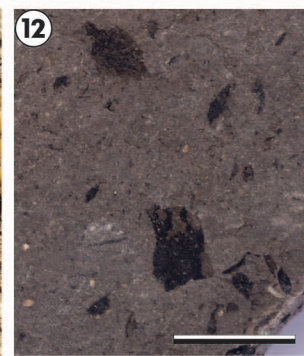
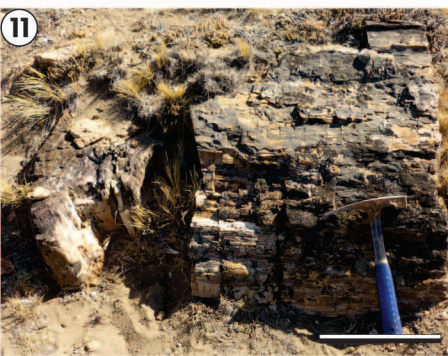
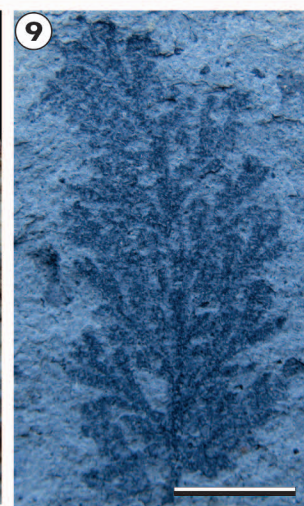
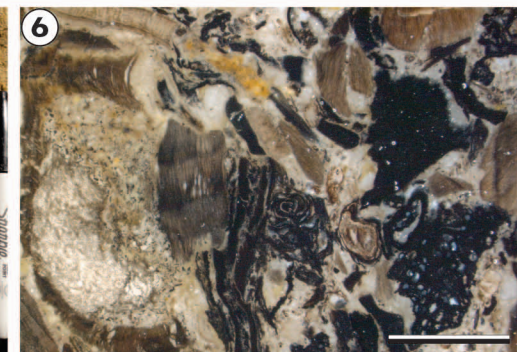
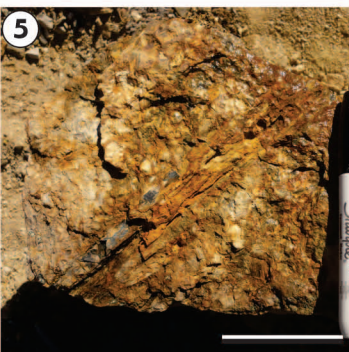
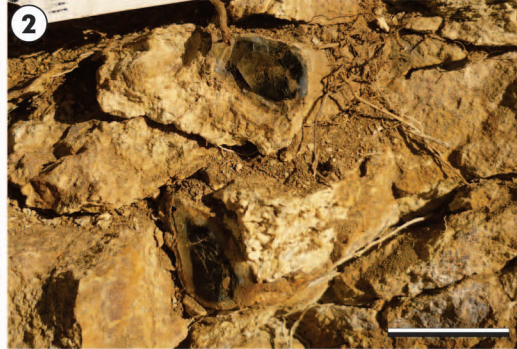
Contacts

- Net
- Unconformity

Fossils

- Impression/compressions
- Permineralized stems
- Carbonized wood
- In situ forest
- Silicified roots
- Casts





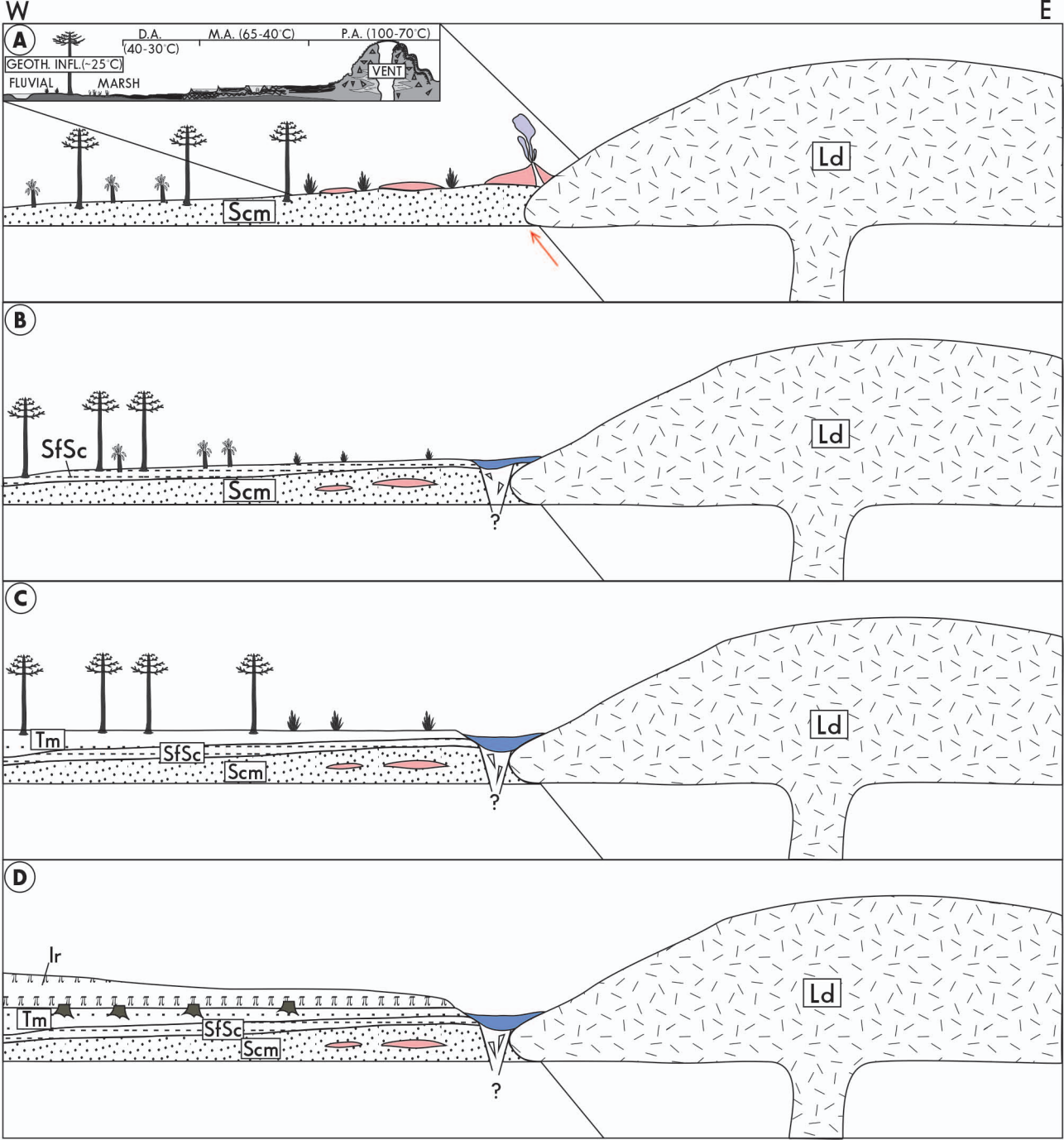


TABLE 1. Facies code for the outcrops of Laguna Flecha Negra locality.

Code	Lithology	Fossil content	Thickness	Geometry	Main features
Ld	Andesitic lava	–	?	Dome	Angular mafic xenoliths. Alteration from degraded biotites to green-blue lavic fragments. Intense weathering at the margins
Scm	White volcanic sandstone	Permineralized roots, impressions and casts of stems, permineralized stems of medium size	12.5 m	Tabular	Coarse grain angular volcanic clasts and eroded feldspar crystals. Massive
Ch	Chert	Abundant Permineralized plant fragments	20 cm	Lenticular	Chert lenses with abundant vegetal detritus distributed in a massive silica matrix, some appear parallel to the chert limits
SfSc	Dark sandstone and siltstone	Well preserved fossil flora of impressions and impression-compressions	10–35 cm	Tabular	Fine grain. Stratification surfaces with strongly weathered volcanic clasts, ash particles and mica flakes. Fining upwards from fine sandstone to siltstone. Cross-lamination that goes parallel at the top of the horizons
Tm	White tuffs	<i>In situ</i> permineralized forest	15 m	Tabular	Coarse to fine grain. Massive, with an upward-fining tendency. End-up in thin lapilli horizons
Ir	Pink rhyolitic ignimbrite	–	12.5 m	Tabular. Thinning to the south	Eutaxitic. Massive structure

TABLE 2. Lithofacies subdivision of the acid Jurassic volcanism of the Deseado Massif.

Bahía Laura Complex	Facies volcanoclastic	Subfacies pyroclastic	Subfacies pyroclastic flow (Ir) Subfacies pyroclastic fall (Scm; Tm) Subfacies pyroclastic surge
		Subfacies epiclastic (Ch; Scm; SfSc)	
	Facies effusive	Subfacies lavic (Ld)	
		Subfacies subvolcanic	

Modified from Guido (2004).
